Cancer Research

Endocan Is Upregulated on Tumor Vessels in Invasive Bladder Cancer Where It Mediates VEGF-A–Induced Angiogenesis

Filip Roudnicky[1], Cedric Poyet[2], Peter Wild[3], Sarah Krampitz[1], Fabrizia Negrini[1], Reto Huggenberger[1], Anja Rogler[4], Robert Stöhr[4], Arndt Hartmann[4], Maurizio Provenzano[2], Vivianne I. Otto[1], and Michael Detmar[1]

Abstract

Tumor-associated blood vessels differ from normal vessels and proteins present only on tumor vessels may serve as biomarkers or targets for antiangiogenic therapy in cancer. Comparing the transcriptional profiles of blood vascular endothelium from human invasive bladder cancer with normal bladder tissue, we found that the endothelial cell-specific molecule endocan (ESM1) was highly elevated on tumor vessels. Endocan was associated with filopodia of angiogenic endothelial tip cells in invasive bladder cancer. Notably, endocan expression on tumor vessels correlated strongly with staging and invasiveness, predicting a shorter recurrence-free survival time in noninvasive bladder cancers. Both endocan and VEGF-A levels were higher in plasma of patients with invasive bladder cancer than healthy individuals. Mechanistic investigations in cultured blood vascular endothelial cells or transgenic mice revealed that endocan expression was stimulated by VEGF-A through the phosphorylation and activation of VEGFR-2, which was required to promote cell migration and tube formation by VEGF-A. Taken together, our findings suggest that disrupting endocan interaction with VEGFR-2 or VEGF-A could offer a novel rational strategy to inhibit tumor angiogenesis. Furthermore, they suggest that endocan might serve as a useful biomarker to monitor disease progression and the efficacy of VEGF-A–targeting therapies in patients with bladder cancer. *Cancer Res; 73(3); 1097–106. ©2012 AACR.*

Introduction

Bladder cancer is the fifth most common cancer in the developed world. It has been estimated that in 2008, 386,300 persons were diagnosed with bladder cancer worldwide and 150,200 succumbed to the disease (1). Bladder cancer has been classified into superficial (pTa, pT1, and CIS) and muscle-invasive (pT2-4) cancer based on whether tumor infiltration extends to the muscular bladder wall (2). However, based on genetic (3) and expression data (4) of bladder cancers of different stages, the revised World Health Organization classification proposes a distinction of noninvasive (pTa) and invasive (pT1-4) bladder cancers. Noninvasive bladder cancers (pTa) have a low risk of progression but a high risk of recurrence. To date, there are no clinical parameters that reliably predict tumor recurrence or progression. Despite the treatment of invasive bladder cancer with radical cystectomy (5), up to 50% of patients develop metastases and 5-year survival is low (6). Increased microvessel density (7) and high expression of VEGF-A correlate with poor prognosis (8), progression (9, 10), and shorter survival of patients with bladder cancer (11). We aimed at elucidating differences at the molecular level between tumor-associated blood vasculature and normal vasculature, which might serve as therapeutic targets or as prognostic biomarkers. Therefore, we isolated blood vascular endothelial cells (BEC) from bladder cancer and normal bladder tissue, using immunolaser capture microdissection (i-LCM), and conducted a comparative microarray expression analysis.

We found that endocan (endothelial cell-specific molecule 1) was one of the most strongly upregulated genes in tumor BECs. Endocan is a secreted proteoglycan (12) that is upregulated by growth factors and chemokines *in vitro* (13, 14) and on tumor vasculature in several types of cancer (15–17), with diverse suggested biologic roles (18). Using quantitative reverse-transcription PCR (qRT-PCR) and immunohistochemistry, we found that endocan was strongly upregulated on tumor vascular endothelium and that its expression correlated with the invasiveness of bladder cancer. Significantly elevated endocan levels were measured in the plasma of patients with invasive bladder cancer compared with healthy individuals. Importantly, we found that VEGF-A induces endocan expression *in vitro* and *in vivo* via VEGF receptor-2 (VEGFR-2) and that endocan knockdown in BECs inhibited VEGF-A–induced tube formation, migration, and VEGFR-2 phosphorylation. Therefore, endocan seems to be an important mediator of

Authors' Affiliations: [1]Institute of Pharmaceutical Sciences, ETH Zurich; Departments of [2]Urology and [3]Pathology, University Hospital Zurich, Zurich, Switzerland; and [4]Department of Urology, University Hospital Erlangen, Erlangen, Germany

Corresponding Author: Michael Detmar, Institute of Pharmaceutical Sciences, Swiss Federal Institute of Technology, ETH Zurich, Wolfgang-Pauli-Str. 10, HCI H303, CH-8093 Zurich, Switzerland. Phone: 41-44-633-7361; Fax: 41-44-633-1364; E-mail: michael.detmar@pharma.ethz.ch

doi: 10.1158/0008-5472.CAN-12-1855

tumor angiogenesis induced via the VEGF-A–VEGFR-2 axis and might serve as a novel biomarker in bladder cancer.

Materials and Methods

Tumor and plasma samples

Clinically annotated frozen and paraffin-embedded tissue samples of bladder cancers and normal bladder tissue as well as plasma samples were obtained from the University Hospital Zurich (Zurich, Switzerland). The tissue collection was approved by the University Hospital Zurich Ethics Committee (SPUK GGU-USZ Ethics Committee KEK-StV-Nr 02/09) and informed written consent was obtained from each patient. Control plasma samples were obtained from healthy blood donors. In addition, we used a bladder cancer tissue microarray (TMA) containing 143 samples from 91 patients (67 male, 24 female; age range, 29–97 years) from the Institute of Pathology, University Hospital Erlangen (Erlangen, Germany). The TMA consisted of 89 papillary noninvasive [pTa and papillary urothelial neoplasms of low malignant potential (PUNLMP)] and 54 invasive (pT1-4) tumors. Blood vessels were identified on the basis of their typical morphology by a board-certified pathologist (P. Wild), and only vessels within tumors were analyzed to reduce heterogeneity. Endocan expression on blood vessels was semiquantitatively assessed by grading the intensity of the staining on the majority of vessels as absent (0), weak (1+; endocan staining weaker than nuclear staining), or strong (2+; endocan staining stronger than nuclear staining). The statistical significance was computed using Fisher's exact test. The Kaplan–Meier log-rank test was used to analyze recurrence-free survival of patients with noninvasive bladder cancer (pTa; $n = 40$) with strong endocan expression versus those with weak or absent endocan expression.

Immunolaser capture microdissection of blood vessels from bladder tissue

Frozen sections of invasive bladder cancer (5 patients; pT1-pT4) and matched normal (tumor-adjacent) bladder tissue were fixed in acetone for 1 minute at 4°C. Blood vessels were stained using biotinylated rabbit anti-human von Willebrand factor (vWF) antibody (0.25 mg/mL; Dako Cytomation) and Cy3-streptavidin (1:100) in a mixture of buffers A and B (all Life Technologies) containing Protector RNase inhibitor (2U/μL; Roche). Slides were dehydrated in 75% ethanol, 95% ethanol, 100% ethanol, and xylene. Immediately afterward, i-LCM was conducted using near infrared-laser–based Arcturus Veritas LCM (Life Technologies). Up to 1 mm^2 of immunostained blood vessels were isolated per sample and immediately lysed in Buffer RLT Plus (Qiagen) containing 3% β-mercaptoethanol.

RNA isolation, cDNA generation, and microarray hybridization of i-LCM samples

RNA was isolated using the RNeasy Plus Micro Kit (Qiagen), amplified and converted to cDNA using the whole transcriptome amplification kit Ovation Pico WTA System (Nugen). Then, cDNA was purified using the QIAquick PCR Purification Kit (Qiagen). Biotin-labeled cDNA targets were hybridized to Human Exon ST 1.0 arrays (Affymetrix) and arrays were scanned according to the manufacturer's protocol. The microarray data are available at Gene Expression Omnibus (GEO) under accession number GSE41614.

Immunohistochemical and immunofluorescent stainings

Paraffin-embedded tissue sections and the TMA were dewaxed in xylene and rehydrated using graded percentages of ethanol. After incubation in 3% H_2O_2 for 10 minutes, sections were boiled in Tris–EDTA buffer, pH 9 for 20 minutes. Staining for endocan and VEGF-A was conducted using mouse anti-human endocan MEP08 antibody (10 μg/mL, Lunginnov) and rabbit anti-human VEGF-A A-20 antibody (4 μg/mL, Santa Cruz). Biotin-labeled horse anti-mouse (5 μg/mL) and biotin-labeled goat anti-rabbit (15 μg/mL) antibodies were used as secondary antibodies. Immunoreactive signals were amplified by formation of avidin–biotin peroxidase complexes and visualized using 3-amino-9-ethylcarbazole (AEC) or 3,3′-diaminobenzidine (DAB). Nuclear counterstaining was conducted with hematoxylin. A rabbit anti-human vWF antibody (15.5 μg/mL) and Alexa Fluor 594-labeled donkey anti-rabbit antibody (1:200) were used for immunofluorescence stainings, followed by Hoechst (10 μg/mL) nuclear staining.

Confocal imaging

Immunofluorescent double staining was conducted on 80-μm thick sections according to ref. (19), using the endocan antibody MEP08 and the vWF antibody, followed by Alexa Fluor 594-labeled donkey anti-mouse (1:500) and Alexa Fluor 488-labeled donkey anti-rabbit (1:500) antibodies. Images were acquired with a Leica SP2 confocal microscope using a 63 × 1.4 NA Plan Apochromat objective with oil immersion lens. Three-dimensional reconstruction was conducted using the Imaris software (Bitplane Scientific Software). The resulting image represents a stack of 47 sections (Z step of 0.244 μm) with a total physical length of 11.23 μm. The voxel height was 0.173 μm with a zoom of 2.693.

ELISA assays

Plasma samples from 60 healthy donors (median, 58 years; range, 36.8–75 years; male, 87%; female, 13%) and 53 patients with invasive bladder cancer (median, 70.8 years; range, 45.3–84 years; male, 79%; female, 21%) were analyzed by ELISA for endocan (Diyek endomark H1; Lunginnov) and VEGF-A (Platinum; eBiosciences), using a Sunrise Tecan microplate reader (Tecan). For BEC lysates, the protein concentration of samples was adjusted, using a bicinchoninic acid assay (Thermo Scientific).

VEGF-A transgenic mice and VEGFR-2–blocking experiments

K14/VEGF-A transgenic (Tg) mice that express mouse VEGF-A164 under control of the K14 promoter (20, 21) were bred and housed in the animal facility of ETH Zurich. Untreated FVB wild-type mice were used as controls. Experiments were carried out in accordance with animal protocol 149/2008 approved by the Kantonales Veterinaeramt Zurich (Zurich, Switzerland). Mouse ears were harvested from 24-week-old VEGF-A Tg mice ($n = 6$) and wild-type mice ($n = 6$) and

homogenized in RLT buffer (RNeasy lysis buffer, Qiagen) containing 1% β-mercaptoethanol. VEGF-A Tg mice (15-weeks old) were also treated with 800 μg of rat anti-mouse VEGFR-2–blocking antibody DC101 (ImClone Systems) or control rat immunoglobulin G (IgG; Sigma) intraperitoneally every other day for 7 days.

Isolation of dermal BECs by fluorescence-activated cell sorting

Dermal BECs were isolated from the ears of VEGF-A Tg mice treated with DC101 ($n = 5$) or control IgG ($n = 3$), and of wild-type FVB mice ($n = 6$) using high-speed cell sorting as described (22).

Cell culture

Primary human dermal BECs (23) and human umbilical vein endothelial cells (HUVEC; Promocell) were seeded onto fibronectin-coated culture dishes (10 μg/mL; BD Biosciences) and were cultured in endothelial cell basal medium (EBM; Lonza) supplemented with 20% FBS (Invitrogen), 2 mmol/L L-glutamine (Fluka), 10 μg/mL hydrocortisone (Fluka), and antibiotic/antimycotic solution (Invitrogen). The BEC media also contained endothelial cell growth supplement (Promocell). Cells of passage 6 to 8 were used.

Cell treatment with proangiogenic factors and VEGFR-2–blocking experiments

Twelve hours before stimulation, media were replaced with EBM containing 1% FBS. Cells were then treated with recombinant human VEGF-A (20 ng/mL) or fibroblast growth factor (FGF)-2 (20 ng/mL; R&D Systems) or both. Cells treated with vehicle were used as controls. For some experiments, cells were preincubated with human monoclonal antibody IMC-1121B against VEGFR-2 (20 μg/mL; ImClone Systems) or with control human IgG for 4 hours, followed by incubation with VEGF-A (20 ng/mL) for 24 hours. Then, cells were washed and lysed in RLT buffer containing 3% β-mercaptoethanol.

RNA isolation and cDNA generation from endothelial cell lysates and mouse ears

RNA was isolated from mouse ear homogenates and from BECs using the RNeasy Mini Kit and treated with RNase-free DNase (all from Qiagen). cDNA was generated from 1 μg RNA using the High-Capacity cDNA Reverse Transcription Kit (Life Technologies).

Quantitative real-time PCR

The expression of mouse and human endocan was quantified by TaqMan RT-PCR with the AB 7900 HT Fast Real-Time PCR System and the $2^{-\Delta\Delta C_t}$ method (24). TaqMan probe/primer sets for mouse (Mm00469953_m1) and human endocan (Hs00199831_m1) and for mouse CD34 (Mm00519283_m1) were predesigned by Life Technologies. Each reaction was multiplexed with β-actin (4326315E) or B2M (4326319E) for human endothelial cells, or β-actin (4352341E, all from Life Technologies) for mouse samples. Expression of endocan and CD34 was normalized to the expression of the reference gene.

siRNA knockdown of endocan

siRNA electroporation of HUVEC was conducted using the Amaxa Basic Nucleofactor Kit for primary endothelial cells (Lonza). The knockdown efficiency of 3 different siRNA constructs against endocan was evaluated (ID: 136192, ID: 19124, ID: 19216). Knockdown using siRNA ID: 136192 showed the strongest reduction of endocan mRNA (data not shown). Therefore, siRNA ID: 136192 and the no. 1 siRNA control nontargeted siRNA (all Ambion) were used. After 24 or 36 hours, supernatants were collected and cells were lysed in RLT buffer containing 3% β-mercaptoethanol, or in a hypotonic PBS solution containing 1 mmol/L $MgCl_2$, 1 mmol/L $CaCl_2$, 1 mmol/L phenylmethanesulfonyl fluoride, and protease inhibitor cocktail (Roche) as described (25).

Western blot analyses

Supernatants were concentrated using a Centricon Ultracel YM-10 membrane filter (Millipore). Proteins were precipitated as described (26). Supernatant samples containing 100 μg of protein and cell lysate samples containing 10 μg of protein (assessed using the BCA protein assay) were subjected to SDS-PAGE using 10% acrylamide separating gels, 1.0 mm. Proteins were transferred to Immobilon-P transfer membranes (Millipore) and stained using a biotinylated goat anti-human endocan antibody (0.2 μg/mL; R&D Systems) or rabbit anti-human (p1175)VEGFR-2 (D55B11; 1:1,000), VEGFR-2 (55B11; 1:1,000), or extracellular signal–regulated kinase (ERK) 1/2 (137F5; 1:1,000; all Cell Signaling) antibodies and a streptavidin-bound horseradish peroxidase conjugate (1:5,000) or horseradish peroxidase–coupled anti-rabbit antibody (1:5,000). Stained proteins were detected using the ECL Plus Western Blotting Detection System (GE Healthcare). Equal loading was confirmed by Ponceau S (Sigma) staining and by staining for vWF (6 μg/mL; ref. 27) or ERK 1/2.

Tube formation and migration assays

The capillary tube formation assay was conducted as described (28) with minor modifications. Matrigel (BD Biosciences) was added to 96-well plates (40 μL per well) and let solidify for 30 minutes at 37°C. HUVECs were electroporated with endocan siRNA or nontargeting siRNA (100 μL of cell suspension containing 15,000 cells/well), seeded on top of Matrigel in sextaplicates and incubated for 12 hours. Images were acquired with a digital camera (AxioCam MRm, Carl Zeiss) mounted on an inverted microscope (Axiovert 200M, Carl Zeiss). The total length of tube-like structures per well was measured using ImageJ. Endothelial cell migration was assessed using a Scratch monolayer wound-healing assay (29). HUVECs were electroporated using endocan siRNA or nontargeting siRNA and seeded into fibronectin-coated wells in quadruplicates (120,000 cells/well). At confluency, 2 cross-shaped scratches were made in each well using a sterile 200-μL pipette tip. Cells were washed and VEGF-A (20 ng/mL) or plain medium were added. Images of crosses were taken immediately and 25 hours later. The surface areas of the cell-free zones were measured and the percentage scratch closure was determined using TScratch software (29).

Statistical analyses

Statistical analyses were conducted using Prism version 5.00 (GraphPad Software, Inc.). For most comparisons, a 2-tailed unpaired Student t test was conducted. The differences in plasma concentrations of VEGF-A and endocan were analyzed with the Mann–Whitney U test. Spearman rank correlations were made to test for the association between endocan and VEGF-A concentrations in plasma. The area under curve (AUC), sensitivity, specificity, positive predictive value (PPV), negative predictive value (NPV), and likelihood ratio were calculated from the receiver operating characteristics (ROC) curve. The comparison between endocan expression in noninvasive and invasive cancers was calculated using Fisher's exact test. Survival data were plotted using the Kaplan–Meier method and analyzed using the log-rank (Mantel–Cox) test. Differences were considered statistically significant at $P < 0.05$.

Results

Endocan expression is upregulated in invasive bladder cancer-associated blood vascular endothelial cells

We isolated endothelial cells from bladder cancer-associated vessels and from vessels in normal surrounding bladder tissue by i-LCM. TaqMan-based qRT-PCR showed that endocan mRNA expression was 1,000- to 100,000-fold higher in tumor-associated BECs than in normal BECs (Fig. 1A). Immunohistochemical staining revealed that the endocan protein was present on tumor-associated blood vessels but not on the blood vessels of normal bladder tissue (Fig. 1B). Confocal imaging of immunofluorescently stained sections of invasive bladder cancer revealed that endocan was associated with the surface of the plasma membrane of BECs. Staining was particularly intense at the filopodia of endothelial tip cells, which typically are vWF-negative (ref. 30; Fig. 1C).

Endocan expression is higher on blood vessels of invasive than noninvasive bladder cancer and is associated with reduced recurrence-free survival

No staining for endocan was detected in normal bladder tissue (Fig. 2A). We next analyzed a TMA consisting of noninvasive ($n = 89$) and invasive bladder cancers ($n = 54$). Of these, 116 samples contained a sufficient number of vessels for analysis of endocan expression, which was semiquantitatively assessed by grading the intensity of the staining as absent (0; Fig. 2B), weak (1+; Fig. 2C), or strong (2+; Fig. 2D). We observed that endocan expression was heterogeneous in individual punches (Fig. 2E). Vessels outside the tumors were negative (Fig. 2F), therefore only vessels within tumors were analyzed to reduce heterogeneity (Fig. 2G). Fifty-three of

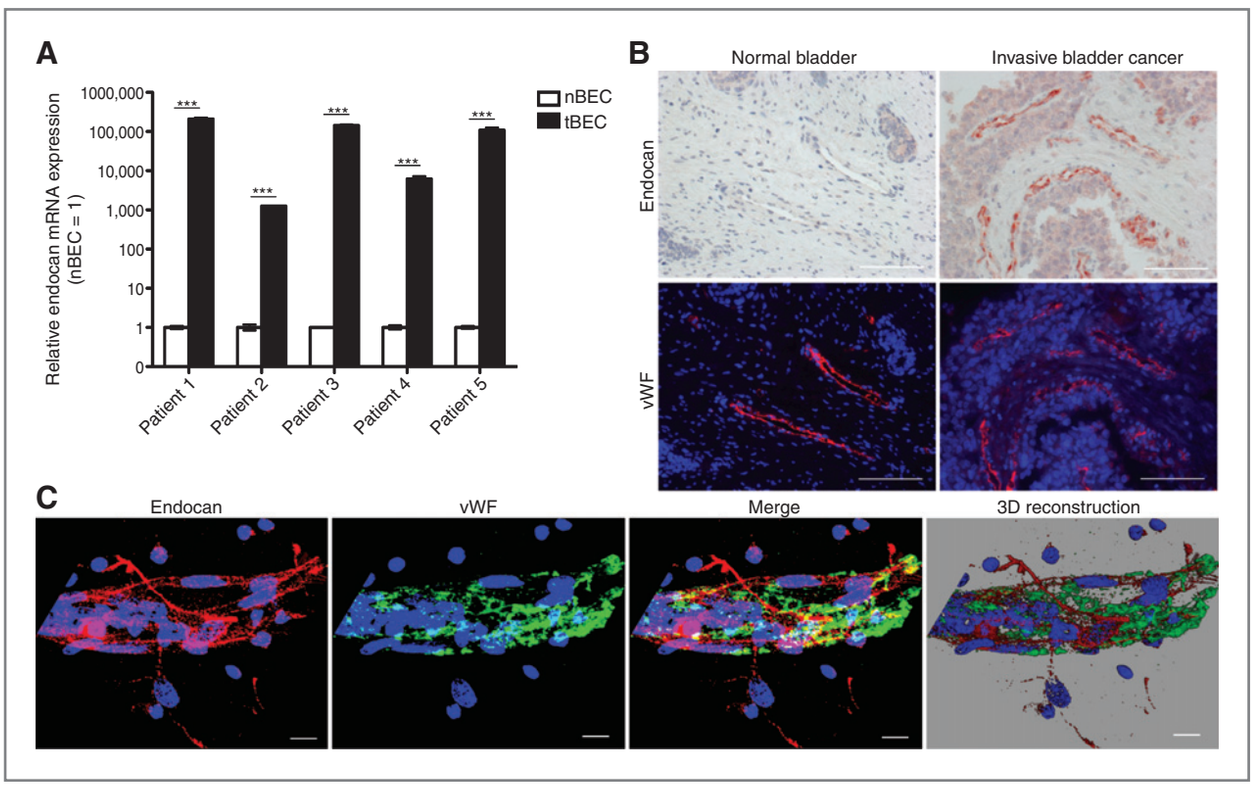

Figure 1. Endocan expression is upregulated in invasive bladder cancer-associated BECs. A, BECs were isolated from frozen sections of invasive tumors (tBEC) and adjacent normal (nBEC) tissue from 5 patients. Endocan mRNA was quantified by qRT-PCR and normalized to the mean expression in nBEC. Data represent mean ± SD. ***, $P < 0.001$. B, paraffin sections of invasive bladder cancer and normal bladder tissue were stained immunohistochemically for endocan (red) and immunofluorescently for vWF as a blood vessel marker, and with hematoxylin or Hoechst (nuclear counterstains). Scale bars, 100 μm. C, z-stack slice of a confocal image of invasive bladder cancer immunofluorescently stained for endocan (red), vWF (green), and Hoechst (blue). Three-dimensional (3D) reconstruction of confocal z-stack using Imaris software. Scale bars, 10 μm.

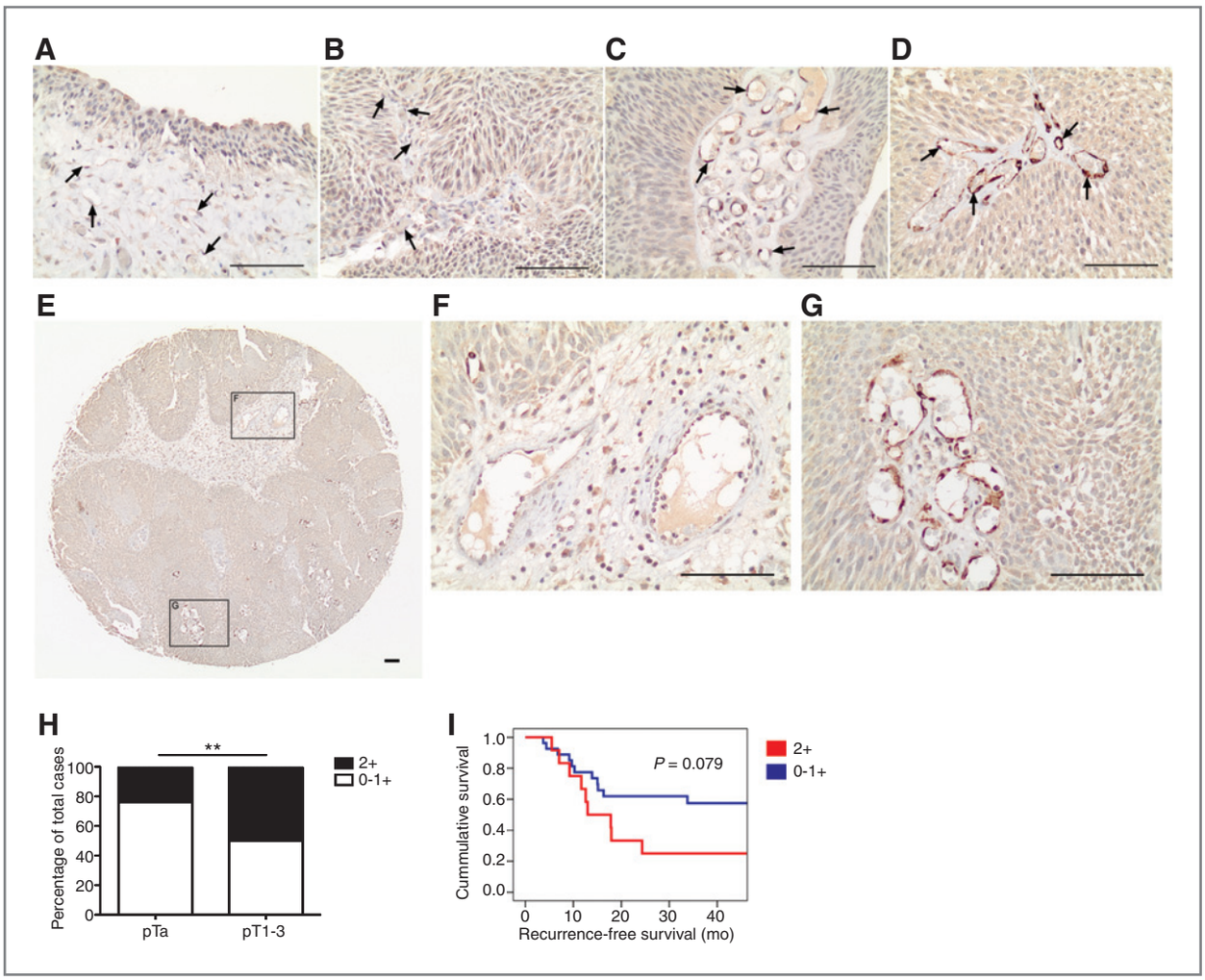

Figure 2. Endocan expression is higher in blood vessels of invasive than noninvasive bladder cancer and is associated with reduced recurrence-free survival. Endocan expression on blood vessels (arrows) was semiquantitatively assessed by grading the staining intensity. Representative images of normal urothelium (A) and of bladder cancers with absent (B), weak (C), and strong (D) endocan expression (brown) are shown. Representative images of a sample TMA core (E), weak endocan expression in the stroma (F), and strong expression in the tumor (G). Scale bars, 100 μm. H, quantification of endocan expression levels in noninvasive (pTa) and invasive (pT1-pT3) bladder cancers of a TMA of 116 bladder cancers. **, $P < 0.01$. I, Kaplan–Meier recurrence-free survival curves of patients with noninvasive bladder cancer (pTa; $n = 40$) with strong endocan expression (2+) versus those with weak or absent endocan expression (0, 1+).

70 samples of noninvasive bladder cancer had no or weak staining for endocan, whereas 17 samples had strong staining. From 46 invasive samples, 23 had no or weak staining and 23 had strong staining. The difference in frequencies between these groups was significant ($P = 0.005$; Fig. 2H), indicating that endocan expression on tumor blood vessels increases with invasiveness of bladder cancer. Kaplan–Meier analysis of 40 samples of pTa cancers showed that patients with strong endocan expression ($n = 12$; $N_{events} = 9$) had a reduced recurrence-free survival compared with those with no or weak endocan expression ($n = 28$; $N_{events} = 14$; $P = 0.079$; Fig. 2I).

Endocan is elevated in plasma of patients with invasive bladder cancer

We next tested whether the increased endocan expression in invasive bladder cancers would also be apparent in plasma. The mean concentration of endocan was significantly higher ($P < 0.001$; Mann–Whitney U test) in the plasma of patients with invasive bladder cancer (0.79 ng/mL; range, 0.23–3.53 ng/mL; $n = 53$) than of healthy volunteers (0.43 ng/mL; range, 0–1 ng/mL; $n = 60$; Fig. 3). Using ROC curve and AUC, we determined the ability of endocan levels to allow for distinction between patients with invasive bladder cancer and healthy subjects. The AUC, sensitivity, and specificity were 0.76, 64%, and 80%, respectively, with a cutoff of 0.63 ng/mL. The PPV and the NPV were 74% and 72%, respectively, with a likelihood ratio of 3.208.

VEGF-A is increased in tumor tissue and plasma of patients with invasive bladder cancer

It has been reported that *in vitro*, endocan expression is induced by VEGF-A (13, 16). We therefore asked whether the

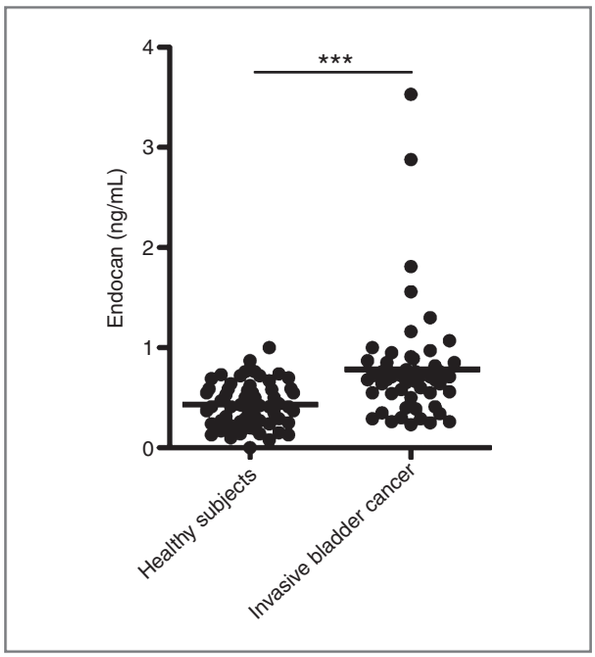

Figure 3. Endocan is elevated in plasma of patients with invasive bladder cancer. Endocan was measured in plasma of patients with invasive bladder cancer ($n = 53$) and in healthy volunteers of similar age ($n = 60$) by ELISA. Dots represent patient samples. Horizontal lines represent mean values. ***, $P < 0.001$.

enhanced endocan expression on tumor blood vessels might be due to increased VEGF-A production. Immunostaining of invasive bladder cancers revealed VEGF-A expression by tumor cells (Fig. 4A, right, white arrows). VEGF-A was also present on tumor-associated blood vessels, likely reflecting VEGF-A bound to its receptors (31; Fig. 4A, right, black arrows). In contrast, VEGF-A was not detected in normal bladder tissue (Fig. 4A, left) and in noninvasive bladder cancer (Fig. 4A, middle). VEGF-A levels in plasma of healthy blood donors were significantly lower (mean, 0.12 ng/mL; range, 0.01–0.4 ng/mL; $n = 60$) than in patients with invasive bladder cancer (mean, 0.28 ng/mL; range, 0.04–0.89 ng/mL; $n = 53$; $P < 0.001$; Mann–Whitney U test; Fig. 4B). The AUC, sensitivity, and specificity were 0.83, 68%, and 90%, respectively, with a cutoff of 0.1895 ng/mL. The PPV and the NPV were 86% and 76%. The likelihood ratio was 6.72. Combining the 113 samples analyzed, we found a significant correlation of VEGF-A and endocan levels ($P = 0.004$; Fig. 4C).

Endocan expression is upregulated by VEGF-A *in vitro* and *in vivo*

After treatment of human BECs with VEGF-A (20 ng/mL) for 24 hours, endocan expression was significantly increased at the mRNA (1.58–1.80-fold; Fig. 5A) and protein level in cell lysates (mean, 10.17; range, 9.48–10.62 ng/mL; control treated: mean, 7.79 ng/mL; range, 6.21–8.73 ng/mL; Fig. 5B). Increased endocan levels were also detected in culture

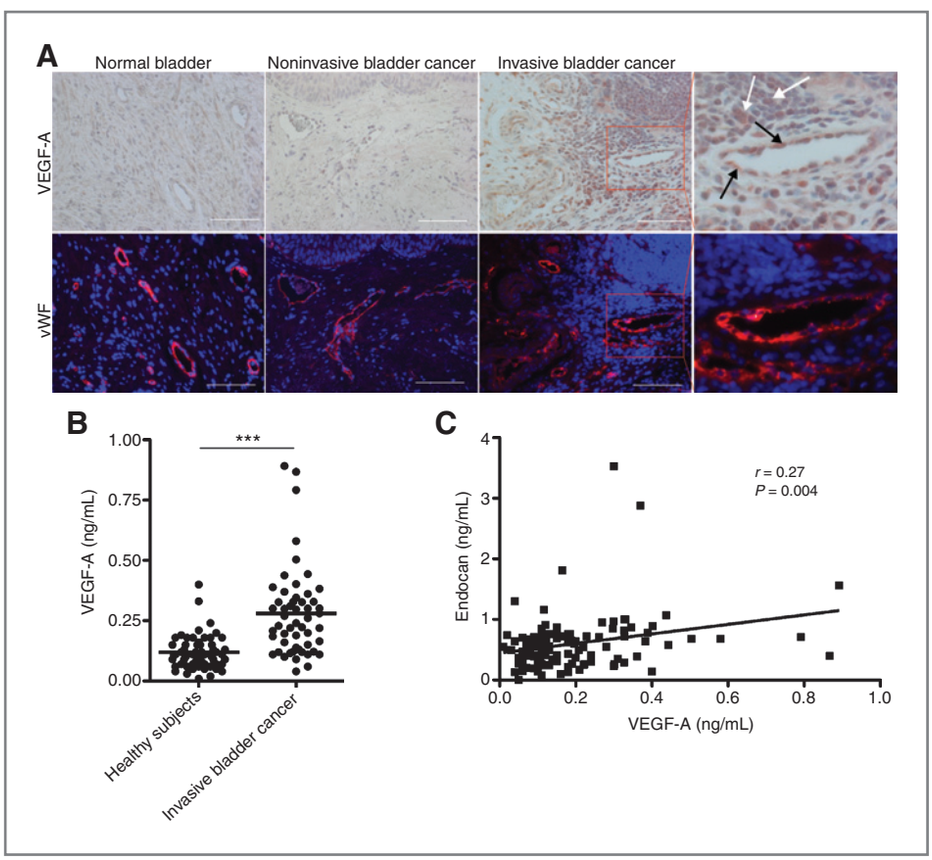

Figure 4. VEGF-A is increased in tumor tissue and plasma of patients with invasive bladder cancer. A, paraffin sections of normal bladder tissue (left), noninvasive (middle), and invasive bladder cancer (right) were stained immunohistochemically for VEGF-A (top; brown), immunofluorescently for vWF (bottom; red), and with hematoxylin or Hoechst (nuclear counterstains). Higher magnification of boxed area shows VEGF-A expressed by tumor cells (white arrows) and VEGF-A associated with tumor endothelium (black arrows). Scale bars, 100 μm. B, VEGF-A was measured in plasma of patients with invasive bladder cancer ($n = 53$) and healthy volunteers of similar age ($n = 60$) by ELISA. Dots represent patient samples. Horizontal lines represent mean values. ***, $P < 0.001$. C, significant correlation of endocan and VEGF-A levels ($n = 113$).

supernatants (mean, 41.2 ng/mL; range, 36.45–44.1 ng/mL; control treated: mean, 33.8 ng/mL; range, 32.52–34.59 ng/mL; Fig. 5C). FGF-2 alone or in combination with VEGF-A did not alter endocan mRNA expression. Pretreatment of BECs with a VEGFR-2–blocking antibody inhibited induction of endocan by VEGF-A at the mRNA (0.74–0.76-fold compared with control IgG; Fig. 5D) and protein level (mean, 30.6 ng/mL in supernatants; range, 29.07–32.55 ng/mL; control IgG treated: mean, 39.42 ng/mL; range, 37.74–40.8 ng/mL; Fig. 5E).

To investigate whether VEGF-A might also enhance endocan expression by BECs *in vivo*, we analyzed skin samples obtained from homozygous VEGF-A Tg mice, which have elevated VEGF-A levels in the skin (21). Endocan mRNA expression was strongly increased (27; 2–67.6-fold; Fig. 5F) in the skin of transgenic mice ($n = 6$) compared with wild-type mice ($n = 6$). To investigate whether this was solely the consequence of increased blood vessel numbers, we specifically isolated blood vessel-derived endothelial cells from the ear skin by fluorescence-activated cell sorting (FACS). We found upregulation of endocan in endothelial cells derived from VEGF-A Tg mice (2.91–5.34-fold; Fig. 5G), whereas expression of the vascular marker CD34 was unchanged (Fig. 5H). Treatment of VEGF-A Tg mice with the VEGFR-2 receptor-blocking antibody DC101 resulted in reduced endocan expression in *ex vivo* isolated endothelial cells compared with the control IgG group (0.2–0.46-fold; Fig. 5I); CD34 expression was not affected (Fig. 5J).

Endocan knockdown in BECs inhibits VEGF-A–induced tube formation, migration, and VEGFR-2 phosphorylation

We next investigated whether and how endocan might contribute to VEGF-A–induced angiogenesis. The biologic functions of proteoglycans often depend on the interactions of their glycosaminoglycan chains with protein ligands, such as cytokines and growth factors (32, 33). Therefore, we investigated whether silencing of endocan would affect VEGF-A effects on endothelial tube formation or migration. Electroporation of HUVECs with endocan siRNA strongly reduced endocan expression at the mRNA (Fig. 6A) and protein levels (Fig. 6B). The total length of tube-like structures formed by HUVECs on growth factor-rich Matrigel was significantly reduced upon endocan knockdown compared with control siRNA (−45%; $P = 0.012$; Fig. 6C). In a monolayer wound-healing ("scratch") assay, migration of HUVECs was not affected by endocan knockdown (data not shown). However, when cells were stimulated with VEGF-A, silencing of endocan abolished the migration-inducing effect of VEGF-A (reduction of wound closure by 53% compared with control siRNA knockdown; $P = 0.007$) to levels observed in non-VEGF-A-treated controls (Fig. 6D and E). Importantly, knockdown of endocan, followed by incubation of HUVECs with VEGF-A for 10 minutes, resulted in a strong reduction of VEGFR-2 phosphorylation, whereas the total amount of VEGFR-2 was unchanged (Fig. 6F). These findings indicate that endocan is necessary for VEGF-A–induced signaling and VEGFR-2 phosphorylation.

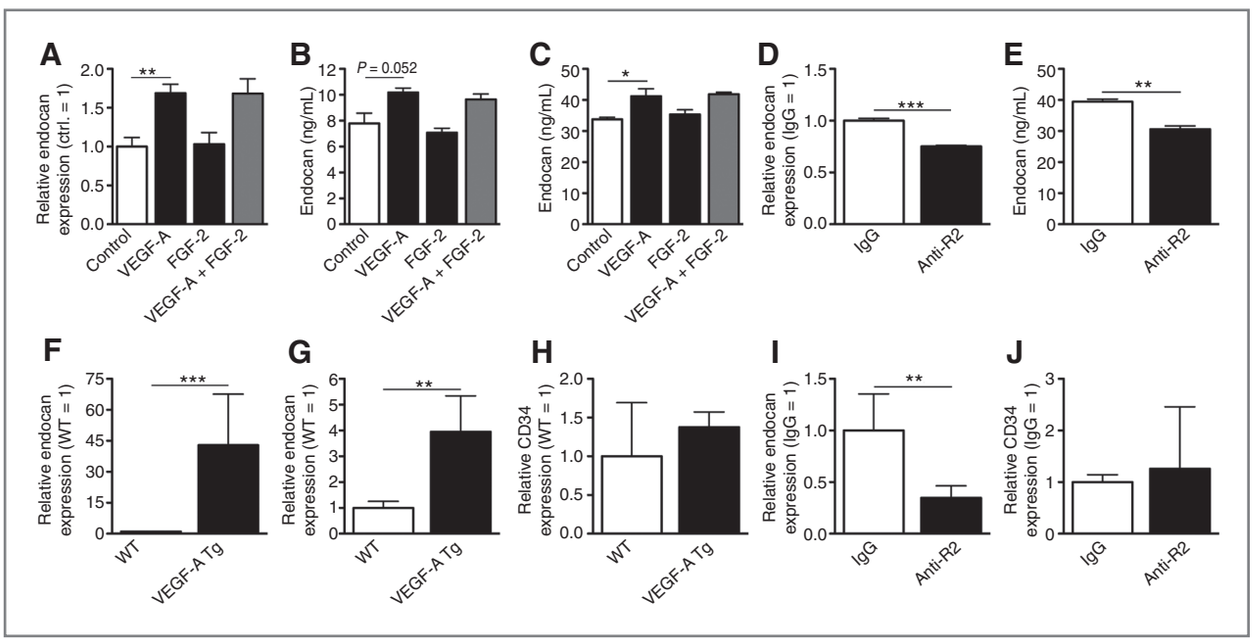

Figure 5. Endocan expression is upregulated by VEGF-A *in vitro* and *in vivo*. Expression of endocan in primary human BECs after incubation with VEGF-A (20 ng/mL) and/or FGF-2 (20 ng/mL) for 24 hours was quantified by qRT-PCR (A) and ELISA in cell lysates (B) and supernatants (C). Cells treated with medium alone were used as controls. Reduced expression of endocan mRNA (D) and protein in supernatants (E) after treatment with a VEGFR-2–blocking antibody. Increased endocan mRNA expression in the skin (F) and in FACS-isolated BECs from skin (G) of homozygous K14-VEGF-A transgenic mice (VEGF-A Tg, $n = 6$) compared with wild-type mice (WT, $n = 6$). CD34 expression levels were comparable in BECs isolated from both genotypes (H). Reduced endocan expression in FACS-isolated BECs from skin of VEGF-A Tg mice ($n = 5$) after treatment with a blocking VEGFR-2 antibody (I), compared with control ($n = 3$). BEC CD34 expression levels were comparable in both treatment groups (J). Data represent mean ± SD. *, $P < 0.05$; **, $P < 0.01$; ***, $P < 0.001$.

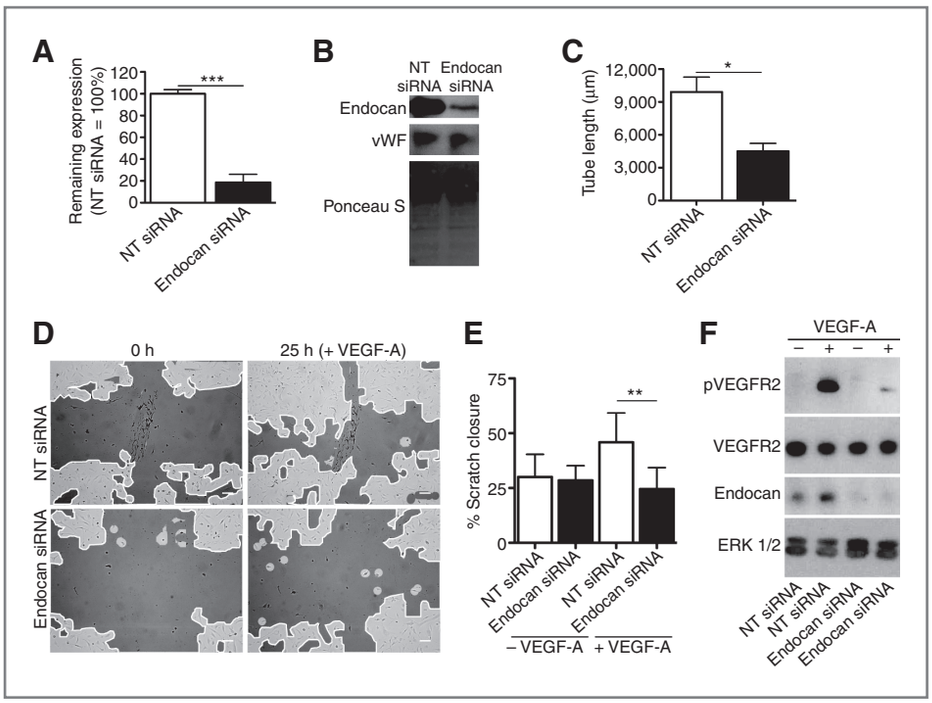

Figure 6. Endocan knockdown in BECs inhibits VEGF-A–induced tube formation, migration, and VEGFR-2 phosphorylation. HUVECs were electroporated with siRNA against endocan or nontargeting siRNA (NT siRNA). Endocan knockdown was confirmed by qRT-PCR (A) and Western blot analysis (B). vWF and Ponceau staining served as loading controls. C, capillary tube formation in VEGF-A containing Matrigel, quantified as total tube length per well in micrometer, was inhibited by endocan siRNA. D, VEGF-A induction of HUVEC migration was prevented by endocan knockdown as assessed in a scratch wound-healing assay. Scale bars, 100 μm. E, quantification of scratch closure ($n = 8$ per group) using TScratch software. Data from 1 representative experiment are presented as mean ± SD. *, $P < 0.05$; **, $P < 0.01$; ***, $P < 0.001$. F, Endocan knockdown potently inhibited VEGFR-2 phosphorylation. HUVECs were incubated with or without VEGF-A for 10 minutes. Cell lysates were subjected to Western blot analysis using anti-phospho-VEGFR-2, anti-VEGFR-2, anti-endocan, and anti-ERK 1/2 antibodies. Staining for ERK1/2 served as a loading control.

Discussion

Here, we established a novel method for efficient isolation of tumor-associated blood vessels from invasive bladder cancers and matched normal bladder tissue using i-LCM. Transcriptional profiling revealed endocan as a gene whose expression was strongly increased on tumor-associated blood vessels, in line with gene expression profiling studies in breast (34), lung (35), and thyroid (36) cancers.

Endocan mRNA and protein expression was strongly increased on blood vessels of invasive bladder cancers compared with normal bladder tissue and noninvasive bladder cancers. Importantly, noninvasive bladder cancer patients with strong endocan expression had a shorter recurrence-free survival than those with absent or weak endocan expression. Currently, the standard follow-up for noninvasive bladder cancer includes cystoscopy combined with cytologic examination at intervals of 3 to 6 months, depending on tumor malignancy and previous recurrence rate. Cystoscopic examinations are unpleasant, time-consuming, expensive, and may have serious side effects, such as infections and damage to the urethra (37). Cytology is characterized by a high specificity but a low sensitivity. So far, there are only few promising molecular markers that might predict recurrence-free survival (38). Our study suggests that endocan might be an additional marker that could allow some prediction how often patients need to undergo cystoscopic examination.

The increased endocan concentrations in the plasma of patients with invasive bladder cancers indicate that endocan might serve as an additional biomarker to evaluate the overall prognosis of invasive bladder cancers. However, additional studies are needed to investigate whether there are consistent differences of plasma endocan levels between invasive and noninvasive cases.

As endocan is a soluble proteoglycan, we asked where it may be localized within the tumor-associated blood vessels. Using high-resolution confocal imaging, we found that endocan was associated with cell membranes of vascular endothelial cells. Particularly high amounts of endocan were associated with filopodia of endothelial cells. Filopodia are typically present on tip cells and are needed for their guidance and motility during angiogenesis (39). In agreement with our findings, expression of endocan was previously also found on tip cells in developing mouse retinas (40, 41).

Tip cells are responsive to VEGF-A and other angiogenic factors and guidance molecules (42), and tumor-associated vessels form extensive filopodia (19). Thus, we asked whether endocan may play a role in migration and sprouting of endothelial cells. Indeed, when endothelial cells were stimulated with VEGF-A, siRNA-mediated endocan silencing abolished

the migration induced by VEGF-A. In contrast to a previous report (43), we found that siRNA-mediated endocan silencing also abolished endothelial tube formation. This discrepancy is likely due to different assay conditions used (HUVECs embedded between 2 layers of collagen gel vs. plating on top of a solidified Matrigel in our study). We also found that expression of endocan by BECs was upregulated after VEGF-A treatment *in vitro*, whereas incubation with FGF-2 had no effect on endocan mRNA or protein production. The different responsiveness of HUVECs (17) and BECs (our study) to FGF-2 likely reflects functional differences between large vessel-derived endothelial cells (HUVEC) and microvasculature-derived endothelial cells (BECs).

Endocan carries a dermatan sulfate chain attached to its serine 137 (18). Dermatan sulfate is a linear polysaccharide, which consists of repeating disaccharide units composed of sulfated N-acetylgalactosamine and either glucuronic or iduronic acid (44). Both the sulfates and the carboxylates of the uronic acids are negatively charged at physiologic pH, thus providing binding sites for signaling molecules comprising positively charged amino acids, such as cytokines and growth factors. Interactions between signaling molecules and glycosaminoglycan chains are often highly specific and may serve to create high local concentrations of signaling molecules, to prolong their half-life by protecting them from proteolytic degradation and to facilitate their binding to their cognate receptors (45). It has been shown that dermatan sulfate chains of endocan bind hepatocyte growth factor (HGF; ref. 46) and promote its mitogenic activity on HEK293 cells (47). However, we previously found that HGF only had a weak effect on the proliferation of BECs (48). In contrast, our novel finding that siRNA-mediated silencing of endocan resulted in strongly reduced phosphorylation of VEGFR-2—the major transmitter of VEGF-A's effects on endothelial cells—upon incubation with VEGF-A, indicates a major role of endocan in mediating the effects of VEGF-A. Endocan is secreted by endothelial cells upon VEGF-A stimulation and binds VEGF-A on the cell surface, facilitating its interaction with VEGFR-2 and increasing the intensity of the VEGF-A signal. It remains to be investigated whether endocan might also have paracrine effects on nonvascular cells (16).

Taken together, these results indicate that VEGF-A induces endocan expression in endothelial cells, which in turn enhances VEGF-A–induced endothelial cell migration and angiogenesis. The interrelation of endocan expression with the presence of VEGF-A on one side and the angiogenesis-inducing function of VEGF-A, supported by endocan, on the other side could make endocan an ideal biomarker for monitoring the therapeutic response to treatment with VEGF-A–targeting antiangiogenic agents. This concept is further supported by the strongly reduced endocan levels after systemic treatment of VEGF-A Tg mice with an anti-VEGFR-2 antibody.

Disclosure of Potential Conflicts of Interest

No potential conflicts of interest were disclosed.

Authors' Contributions

Conception and design: F. Roudnicky, V.I. Otto, M. Detmar
Development of methodology: F. Roudnicky
Acquisition of data (provided animals, acquired and managed patients, provided facilities, etc.): F. Roudnicky, C. Poyet, P. Wild, S. Krampitz, R. Huggenberger, A. Rogler, A. Hartmann, M. Provenzano
Analysis and interpretation of data (e.g., statistical analysis, biostatistics, computational analysis): F. Roudnicky, C. Poyet, P. Wild, S. Krampitz, F. Negrini, A. Rogler, V.I. Otto, M. Detmar
Writing, review, and/or revision of the manuscript: F. Roudnicky, R. Huggenberger, A. Rogler, R. Stöhr, A. Hartmann, M. Provenzano, V.I. Otto, M. Detmar
Administrative, technical, or material support (i.e., reporting or organizing data, constructing databases): F. Roudnicky, C. Poyet, P. Wild, A. Rogler, R. Stöhr, A. Hartmann
Study supervision: M. Detmar

Acknowledgments

The authors thank Sabrina Petsch and Stefan Schick, Tumorzentrum Erlangen, for providing follow-up patient data, Dr. Martin Schulz for help with the scratch assay, Dr. Maija Hollmén and Sinem Karaman for helpful discussions, and Jeannette Scholl and Peter Camenzind for excellent technical assistance.

Grant Support

This work was supported by Swiss National Science Foundation grants 3100A0–108207 and 31003A_130627, Advanced European Research Council Grant LYVICAM, Krebsliga Schweiz and Krebsliga Zurich (to M. Detmar). The TMA construction was supported by a grant from the Interdisciplinary Center for Clinical Research (IZKF), University Hospital Erlangen.

The costs of publication of this article were defrayed in part by the payment of page charges. This article must therefore be hereby marked *advertisement* in accordance with 18 U.S.C. Section 1734 solely to indicate this fact.

Received May 10, 2012; revised December 5, 2012; accepted December 9, 2012; published OnlineFirst December 14, 2012.

References

1. Jemal A, Bray F, Center MM, Ferlay J, Ward E, Forman D. Global cancer statistics. CA Cancer J Clin 2011;61:69–90.
2. Raghavan D, Shipley WU, Garnick MB, Russell PJ, Richie JP. Biology and management of bladder cancer. N Engl J Med 1990;322:1129–38.
3. Eble JN, Sauter G, Epstein JI, Sesterhenn IA, editors. World Health Organization classification of tumours. Pathology and genetics of tumours of the urinary system and male genital organs. Lyon, France: IARC Press; 2004.
4. Wild PJ, Herr A, Wissmann C, Stoehr R, Rosenthal A, Zaak D, et al. Gene expression profiling of progressive papillary noninvasive carcinomas of the urinary bladder. Clin Cancer Res 2005;11:4415–29.
5. Stein JP, Lieskovsky G, Cote R, Groshen S, Feng AC, Boyd S, et al. Radical cystectomy in the treatment of invasive bladder cancer: long-term results in 1,054 patients. J Clin Oncol 2001;19:666–75.
6. Ghoneim MA, el-Mekresh MM, el-Baz MA, el-Attar IA, Ashamallah A. Radical cystectomy for carcinoma of the bladder: critical evaluation of the results in 1,026 cases. J Urol 1997;158:393–9.
7. Bochner BH, Cote RJ, Weidner N, Groshen S, Chen SC, Skinner DG, et al. Angiogenesis in bladder cancer: relationship between microvessel density and tumor prognosis. J Natl Cancer Inst 1995;87:1603–12.
8. Bernardini S, Fauconnet S, Chabannes E, Henry PC, Adessi G, Bittard H. Serum levels of vascular endothelial growth factor as a prognostic factor in bladder cancer. J Urol 2001;166:1275–9.
9. Goddard JC, Sutton CD, Furness PN, O'Byrne KJ, Kockelbergh RC. Microvessel density at presentation predicts subsequent muscle invasion in superficial bladder cancer. Clin Cancer Res 2003;9:2583–6.
10. Crew JP, O'Brien T, Bradburn M, Fuggle S, Bicknell R, Cranston D, et al. Vascular endothelial growth factor is a predictor of relapse and stage progression in superficial bladder cancer. Cancer Res 1997;57:5281–5.
11. Dickinson AJ, Fox SB, Persad RA, Hollyer J, Sibley GN, Harris AL. Quantification of angiogenesis as an independent predictor of prognosis in invasive bladder carcinomas. Br J Urol 1994;74:762–6.

12. Lassalle P, Molet S, Janin A, Heyden JV, Tavernier J, Fiers W, et al. ESM-1 is a novel human endothelial cell-specific molecule expressed in lung and regulated by cytokines. J Biol Chem 1996;271:20458–64.
13. Shin JW, Huggenberger R, Detmar M. Transcriptional profiling of VEGF-A and VEGF-C target genes in lymphatic endothelium reveals endothelial-specific molecule-1 as a novel mediator of lymphangiogenesis. Blood 2008;112:2318–26.
14. Rennel E, Mellberg S, Dimberg A, Petersson L, Botling J, Ameur A, et al. Endocan is a VEGF-A and PI3K regulated gene with increased expression in human renal cancer. Exp Cell Res 2007;313:1285–94.
15. Leroy X, Aubert S, Zini L, Franquet H, Kervoaze G, Villers A, et al. Vascular endocan (ESM-1) is markedly overexpressed in clear cell renal cell carcinoma. Histopathology 2010;56:180–7.
16. Grigoriu BD, Depontieu F, Scherpereel A, Gourcerol D, Devos P, Ouatas T, et al. Endocan expression and relationship with survival in human non–small cell lung cancer. Clin Cancer Res 2006;12:4575–82.
17. Maurage C-A, Adam E, Minéo J-F, Sarrazin S, Debunne M, Siminski R-M, et al. Endocan expression and localization in human glioblastomas. J Neuropathol Exp Neurol 2009;68:633–41.
18. Sarrazin S, Adam E, Lyon M, Depontieu F, Motte V, Landolfi C, et al. Endocan or endothelial cell specific molecule-1 (ESM-1): a potential novel endothelial cell marker and a new target for cancer therapy. Biochim Biophys Acta 2006;1765:25–37.
19. Baluk P, Morikawa S, Haskell A, Mancuso M, McDonald DM. Abnormalities of basement membrane on blood vessels and endothelial sprouts in tumors. Am J Pathol 2003;163:1801–15.
20. Kunstfeld R, Hirakawa S, Hong Y-K, Schacht V, Lange-Asschenfeldt B, Velasco P, et al. Induction of cutaneous delayed-type hypersensitivity reactions in VEGF-A transgenic mice results in chronic skin inflammation associated with persistent lymphatic hyperplasia. Blood 2004;104:1048–57.
21. Xia YP, Li B, Hylton D, Detmar M, Yancopoulos GD, Rudge JS. Transgenic delivery of VEGF to mouse skin leads to an inflammatory condition resembling human psoriasis. Blood 2003;102:161–8.
22. Huggenberger R, Siddiqui SS, Brander D, Ullmann S, Zimmermann K, Antsiferova M, et al. An important role of lymphatic vessel activation in limiting acute inflammation. Blood 2011;117:4667–78.
23. Hirakawa S, Hong Y-K, Harvey N, Schacht V, Matsuda K, Libermann T, et al. Identification of vascular lineage-specific genes by transcriptional profiling of isolated blood vascular and lymphatic endothelial cells. Am J Pathol 2003;162:575–86.
24. Schmittgen TD, Livak KJ. Analyzing real-time PCR data by the comparative C(T) method. Nat Protoc 2008;3:1101–8.
25. Schulz MM, Reisen F, Zgraggen S, Fischer S, Yuen D, Kang GJ, et al. Phenotype-based high-content chemical library screening identifies statins as inhibitors of *in vivo* lymphangiogenesis. Proc Natl Acad Sci USA 2012;109:2665–74.
26. Wessel D, Flügge UI. A method for the quantitative recovery of protein in dilute solution in the presence of detergents and lipids. Anal Biochem 1984;138:141–3.
27. Bignon M, Pichol-Thievend C, Hardouin J, Malbouyres M, Brechot N, Nasciutti L, et al. Lysyl oxidase-like protein-2 regulates sprouting angiogenesis and type IV collagen assembly in the endothelial basement membrane. Blood 2011;118:3979–89.
28. McGonigle S, Shifrin V. *In vitro* assay of angiogenesis: inhibition of capillary tube formation. Current protocols in pharmacology. Hoboken, NJ, USA: John Wiley & Sons, Inc.; 2008.
29. Geback T, Schulz MM, Koumoutsakos P, Detmar M. TScratch: a novel and simple software tool for automated analysis of monolayer wound healing assays. Biotechniques 2009;46:265–74.
30. Magnusson P, Rolny C, Jakobsson L, Wikner C, Wu Y, Hicklin DJ, et al. Deregulation of Flk-1/vascular endothelial growth factor receptor-2 in fibroblast growth factor receptor-1-deficient vascular stem cell development. J Cell Sci 2004;117:1513–23.
31. van der Loos CM, Meijer-Jorna LB, Broekmans ME, Ploegmakers HP, Teeling P, de Boer OJ, et al. Anti-human vascular endothelial growth factor (VEGF) antibody selection for immunohistochemical staining of proliferating blood vessels. J Histochem Cytochem 2009;58:109–18.
32. Hardingham TE, Fosang AJ. Proteoglycans: many forms and many functions. FASEB J 1992;6:861–70.
33. Bishop JR, Schuksz M, Esko JD. Heparan sulphate proteoglycans fine-tune mammalian physiology. Nature 2007;446:1030–7.
34. van 't Veer LJ, Dai H, van de Vijver MJ, He YD, Hart AAM, Mao M, et al. Gene expression profiling predicts clinical outcome of breast cancer. Nature 2002;415:530–6.
35. Borczuk AC, Shah L, Pearson GD, Walter KL, Wang L, Austin JH, et al. Molecular signatures in biopsy specimens of lung cancer. Am J Respir Crit Care Med 2004;170:167–74.
36. Wattel S, Mircescu H, Venet D, Burniat A, Franc B, Frank S, et al. Gene expression in thyroid autonomous adenomas provides insight into their physiopathology. Oncogene 2005;24:6902–16.
37. Van Tilborg AA, Bangma CH, Zwarthoff EC. Bladder cancer biomarkers and their role in surveillance and screening. Int J Urol 2009;16:23–30.
38. Brems-Eskildsen AS, Zieger K, Toldbod H, Holcomb C, Higuchi R, Mansilla F, et al. Prediction and diagnosis of bladder cancer recurrence based on urinary content of hTERT, SENP1, PPP1CA, and MCM5 transcripts. BMC Cancer 2010;10:646.
39. De Smet F, Segura I, De Bock K, Hohensinner PJ, Carmeliet P. Mechanisms of vessel branching: filopodia on endothelial tip cells lead the way. Arterioscler Thromb Vasc Biol 2009;29:639–49.
40. Del Toro R, Prahst C, Mathivet T, Siegfried G, Kaminker JS, Larrivee B, et al. Identification and functional analysis of endothelial tip cell-enriched genes. Blood 2010;116:4025–33.
41. Strasser GA, Kaminker JS, Tessier-Lavigne M. Microarray analysis of retinal endothelial tip cells identifies CXCR4 as a mediator of tip cell morphology and branching. Blood 2010;115:5102–10.
42. Gerhardt H, Golding M, Fruttiger M, Ruhrberg C, Lundkvist A, Abramsson A, et al. VEGF guides angiogenic sprouting utilizing endothelial tip cell filopodia. J Cell Biol 2003;161:1163–77.
43. Aitkenhead M, Wang S-J, Nakatsu MN, Mestas J, Heard C, Hughes CCW. Identification of endothelial cell genes expressed in an *in vitro* model of angiogenesis: induction of ESM-1, βig-h3, and NrCAM. Microvasc Res 2002;63:159–71.
44. Taylor KR, Gallo RL. Glycosaminoglycans and their proteoglycans: host-associated molecular patterns for initiation and modulation of inflammation. FASEB J 2006;20:9–22.
45. Zhang L. Glycosaminoglycan (GAG) biosynthesis and GAG-binding proteins. Prog Mol Biol Transl Sci 2010;93:1–17.
46. Sarrazin S, Lyon M, Deakin JA, Guerrini M, Lassalle P, Delehedde M, et al. Characterization and binding activity of the chondroitin/dermatan sulfate chain from Endocan, a soluble endothelial proteoglycan. Glycobiology 2010;20:1380–8.
47. Bechard D, Gentina T, Delehedde M, Scherpereel A, Lyon M, Aumercier M, et al. Endocan is a novel chondroitin sulfate/dermatan sulfate proteoglycan that promotes hepatocyte growth factor/scatter factor mitogenic activity. J Biol Chem 2001;276:48341–9.
48. Kajiya K, Hirakawa S, Ma B, Drinnenberg I, Detmar M. Hepatocyte growth factor promotes lymphatic vessel formation and function. EMBO J 2005;24:2885–95.